References

[1] Hadlock, C.R., "Singular Perturbations of a Class of Two Point Boundary Value Problems Arising in Optimal Control," Coordinated Science Lab. Rept. R-481, Univ. Illinois, July 1970.

[2] Freedman, M.I., and Kaplan, J.L., "Singular Perturbations of Two-Point Boundary Value Problems Arising in Optimal Control," *SIAM Journal of Control and Optimization,* Vol. 14, Feb. 1976, pp. 189-215.

[3] Aiken, R.C., and Lapidus, L., "An Effective Numerical Integration Method for Typical Stiff Systems," *AIChE Journal,* Vol. 20, March 1974, pp. 368-375.

[4] Ardema, M.D., "Characteristics of the Boundary-Layer Equations of the Minimum Time-to-Climb Problem," *Proceedings of the Fourteenth Annual Allerton Conference on Circuit and System Theory,* Sept. 29, 1976.

[5] Ardema, M.D., "Singular Perturbations in Flight Mechanics," NASA TM X-62, 380, Aug. 1974; revised July 1977.

[6] Ardema, M.D., "Solution of the Minimum Time-to-Climb Problem by Matched Asymptotic Expansions," *AIAA Journal,* Vol. 14, July 1976, pp. 843-850

Valve Delay Effects on Bending Limit Cycles of a Deadband System

Franklin C. Loesch*

The Aerospace Corporation, El Segundo Calif.

REFERENCE 1† contains an analysis of the interactions of a deadband control system with a flexible spacecraft. A simple analytic criterion is developed which determines whether or not it is possible to obtain unstable bending limit cycles—i.e. limit cycles in which both sets of nozzles fire at approximately the bending frequency and in such phase as to expend control gas rapidly for the nonuseful purpose of maintaining a large bending amplitude. This criterion was verified by digital simulation computations.

Of the several simplifying idealizations made in Ref. 1, it is believed that the assumption of equal on and off solenoid valve delays introduces the greatest differences between the analysis predictions and the behavior of a real system. The analysis of this Note therefore supplements Ref. 1 by replacing the assumption of equal on and off delays with more realistic assumptions. Figure 1 is derived from test data on a representative solenoid valve which was subjected to electrical commands of varying duration. The chamber pressure was measured in a small plenum downstream of the valve and upstream of the nozzle. The data records show 1) time of applied voltage on, 2) time of voltage off, 3) pressure history vs time. The latter exhibits a delay after voltage on, then a sloped rise to a level plateau pressure which holds for a time after voltage off, then falls along a slope to zero. The time difference between voltage on and off is called C and is plotted on the horizontal axis of Fig. 1 as the "Voltage Command Interval." Let the plateau pressure be P, the total integral of pressure vs time be I, and the integral after voltage off be I_{off}. The square points on Fig. 1 are (I_{off}/P) and the circle points are $C-[(I-I_{\text{off}})/P]$. Using the idealization of

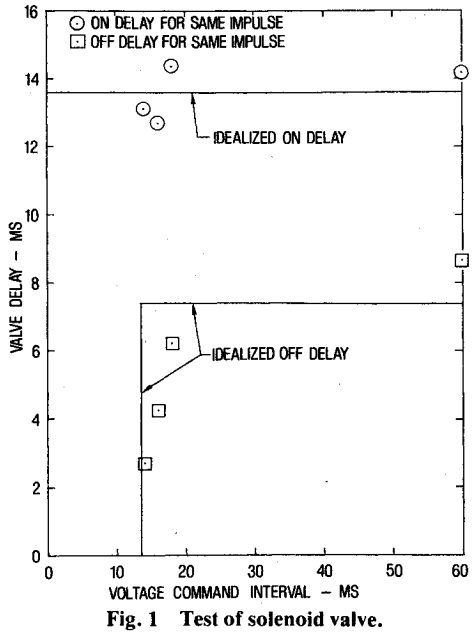

Fig. 1 Test of solenoid valve.

instantaneous rise and fall, the points represent the equivalent delays which result in the same total impulse and same impulse after off command as the real valve exhibits. It is seen that the assumption of a constant on delay is reasonably in accord with the test data. The assumption of constant off delay for commands longer than ~15 ms is less accurate but still fairly reasonable. The assumption that the on delay is equal to the off delay is much less reasonable. The graphical estimates drawn on Fig. 1 give a value of ~13.6 ms for on but only ~7.4 ms for off delay. Thus the assumption of equal on and off delays will result in thrust pulses that are always (13.6 − 7.4) = 6.2 ms too long; and any average value which is chosen for the equal on or off delay cannot represent the true value of on delay for which no thrust occurs. A much more accurate representation is obtained by defining the on and off delays as:

$t_1 = t_{\text{on}} = 13.6$ ms = constant
$t_3 = t_{\text{off}} = 0$ for voltage command interval $\leq t_{\text{on}}$
$t_3 = t_{\text{off}} = 7.4$ ms for voltage command interval $> t_{\text{on}}$

The use of these assumptions results in thrust pulses of approximately the true length and impulse for command lengths greater than t_{on}; but for command lengths less than or equal to t_{on} no thrust occurs, which is approximately in accord with the test data. Evidently a much superior analytic representation for the valve is obtained by allowing on and off delays to be unequal.

The analysis of Ref. 1 is unchanged through Eq. (19); Eq. (20), however, must be replaced by

$$\Delta\psi_{\text{on}} = \tan^{-1}\omega_1 t_2 + \phi + \omega_1 t_1 \qquad \text{(20a rev)}$$

$$\Delta\psi_{\text{off}} = \tan^{-1}\omega_1 t_2 + \phi + \omega_1 t_3 \qquad \text{(20b rev)}$$

Equations (21a) and (21c) are still valid. The work/energy Eq. (26) derivation is identical except that $\Delta\psi$ in all lower integration limits is replaced by $\Delta\psi_{\text{on}}$ and in all upper limits by $\Delta\psi_{\text{off}}$. Then a revised Eq. (43) is obtained from Eq. (26) by the same assumption. The results of the nozzle work integration are conveniently expressed in terms of the average and the difference of the valve on and off delays. Thus with

$$\Delta\psi \equiv \tan^{-1}\omega_1 t_2 + \phi + \tfrac{1}{2}\omega_1 (t_1 + t_3) \qquad \text{(20c)}$$

$$S_1 \equiv \sin[\tfrac{1}{2}\omega_1 (t_1 - t_3)] \qquad \text{(20d)}$$

Received March 5, 1979; revision received June 4, 1979.

Index categories: Spacecraft Dynamics and Control; LV/M Dynamics and Control.

*Director of Program Management Support, Reentry System Division.

†Equations in this note are numbered to correspond to the equations in Ref. 1.

$$C_1 \equiv \cos[\tfrac{1}{2}\omega_1 (t_1 - t_3)] \tag{20e}$$

we obtain with the aid of trigonometric identities

$$\frac{\omega_1}{\omega}\frac{1}{2\pi\zeta}\frac{\Delta P}{A} = -Q\left[C_1 \sin\frac{F_1}{2} - S_1 \cos\frac{F_1}{2}\right]\cos\Delta\psi - \frac{P}{A} \tag{43rev}$$

Expressions for $\sin(F_1/2)$ and $\cos(F_1/2)$ in terms of P'/A and E_{avg}/A are obtained by taking the sine and cosine of both sides of Eq. (19), the definition of F_1. By substituting these expressions into Eq. (43 rev) and relating P' to P through the gain G, we obtain a work/energy equation in the variables P'/A and E_{avg}/A. From this equation P'/A may be eliminated by using Eq. (46) for the double-firing boundary. By retaining unchanged the definition for the parameter B in Eq. (49), the revised function f in Eqs. (48 rev) and (49 rev) thus becomes, with $C = \cos(\omega_1 t_1/2)$ for convenience,

$$f_{rev} = \frac{(C + \sin B)(C_1^2 - \sin^2 B)}{2(S_1 \sin B + C_1 \cos B)} \tag{49 rev}$$

We require the maximum value of f_{rev} in order to obtain the double-firing boundary equation for nonequal on and off valve delays. By taking the derivative of Eq. (49 rev) with respect to B and equating it to zero we obtain a revised Eq. (50) which defines the value of $B = B_1$ at which the maximum value of f_{rev} occurs:

$$C[C_1 \sin B_1 (S_1^2 + \cos^2 B_1) + S_1 \cos B_1 (C_1^2 + \sin^2 B_1)]$$
$$+ C_1[\sin^2 B_1 (1 + 2\cos^2 B_1) - C_1^2] + 2S_1 \sin^3 B_1 \cos B_1 = 0 \tag{50 rev}$$

Equation (50 rev) can be solved by a simple trial numerical procedure to determine B_1; then $(f_{rev})_{max}$ is calculated by substituting B_1 into Eq. (49 rev). The double-firing boundary equation then becomes

$$Q = -\frac{1}{G\cos\Delta\psi\,(f_{rev})_{max}} \tag{52 rev}$$

Finally, the disturbance torque which maximizes the probability of double-firing is still obtained by Eq. (53) of Ref. 1, except that B_1 is now the value determined by Eq. (50 rev). The derivation of Eqs. (41) and (42) for the steady-state limit cycle frequency remains the same, except that the angle $\Delta\psi$ must now be taken as the average phase lag angle given by Eq. (20c) above. Since the nozzle thrust is no longer at a fixed phase angle, the frequency predicted by Eqs. (41) or (42) may be slightly less accurate; however, there appears to be no alternative to the use of the average phase lag, and usually the frequency shift is of only minor importance.

In order to illustrate the differences in the bending oscillation growth caused by nonequal valve on and off delays, Fig. 2 shows zero growth contours of P'/A vs E_{avg}/A. For a chosen value of F_1, Eq. (43 rev) with $\Delta P = 0$ and $P' = GP$ determines a value of P'/A. A value of F_1, however, by Eq. (19) defines a straight line locus in P'/A vs E_{avg}/A coordinates; hence a point on the contour is determined. By choosing several values of F_1 the contour is mapped. For the solid contour of Fig. 2, $t_1 = 13.6$ ms and $t_3 = 7.4$ ms; for the dashed contour $t_1 = t_3 = 10.5$ ms. Thus both contours have the same average delay. Correspondingly the solid double-firing boundary is calculated using the on delay of 13.6 ms, while

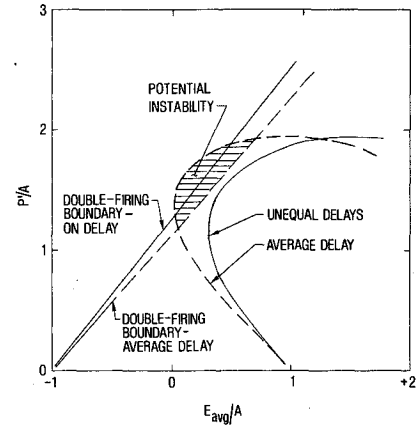

Fig. 2 Bending oscillation zero growth contours.

the dashed boundary uses the average delay. The other input values which apply to Fig. 2 are: $\omega = 15.29$ Hz, $\omega_1 = 15.35$ Hz, $\zeta = 0.10$, $\zeta_g = 0.5$, $\omega_{ng} = 21$ Hz, $t_2 = 0.01$, $Q = 2.5$. Resulting intermediate values are $G = 0.831$ and $\Delta\psi = 159.4$ deg. It is seen for these cases that if the difference between on and off delays were ignored and the method of Ref. 1 was applied using the average delay, the system would be predicted to be unstable because the dashed zero-growth contour extends beyond the corresponding dashed double-firing boundary line. In this case the system would be predicted to be unstable even if the dashed contour, based on average delay, were compared with the solid double-firing boundary line for the on delay. The system is, however, stable because the zero-growth solid contour, which takes account of the difference between on and off delays, does not cross the corresponding solid double-firing boundary. Thus Fig. 2 illustrates that significant differences in stability predictions can arise from neglect of on and off valve delay differences.

By adopting ω_{ng} (the rate gyro's undamped natural frequency) as the unit of frequency the value of Q, the system's nondimensional torque parameter, as determined by the revised double-firing boundary Eq. (52 rev), becomes a function of the following nondimensional parameters:

ζ = structural damping coefficient
ζ_g = rate gyro damping coefficient
$\omega_{ng} t_2$ = nondimensional filter time constant
$\omega_{ng} t_1$ = nondimensional solenoid on delay
$\omega_{ng} t_3$ = nondimensional solenoid off delay
ω/ω_{ng} = ratio of bending natural frequency to rate gyro undamped natural frequency

Figure 3 shows on the vertical axis the absolute value of the boundary value of Q as calculated by Eq. (52 rev) vs the frequency ratio ω/ω_{ng} on the horizontal scale. The variation of the angle $\Delta\psi$ is indicated also on the horizontal scale. Parameter values which apply to Fig. 3 are: $\zeta = 0.01$, $\zeta_g = 0.5$, $\omega_{ng} t_2 = 1$, $\omega_{ng}(t_1 + t_3)/2 = 135$ deg, and $\omega_{ng}(t_1 - t_3) = 0$, 45, and 90 deg. The boundary curves of Fig. 3 are broken into three regions by two vertical asymptotes at values of $\Delta\psi = 90$ and 270 deg. Since $\cos\Delta\psi = 0$ at these values of $\Delta\psi$, the boundary value of Q becomes infinite. The right-hand region is actually bounded by a third asymptote at a frequency ratio of ~ 1.97 which lies off the scale of the figure. The third asymptote is determined by whichever occurs first: $\Delta\psi = 450$ deg, $\cos\Delta\psi = 0$; or by $\omega_1 t_1 = 360$ deg, which makes $f_{max} = 0$. In the left-hand and right-hand regions the boundary value of Q is negative, while in the middle region it is positive. Q is positive or negative depending on the algebraic sign of the product of the modal slope and modal deflection parameters,

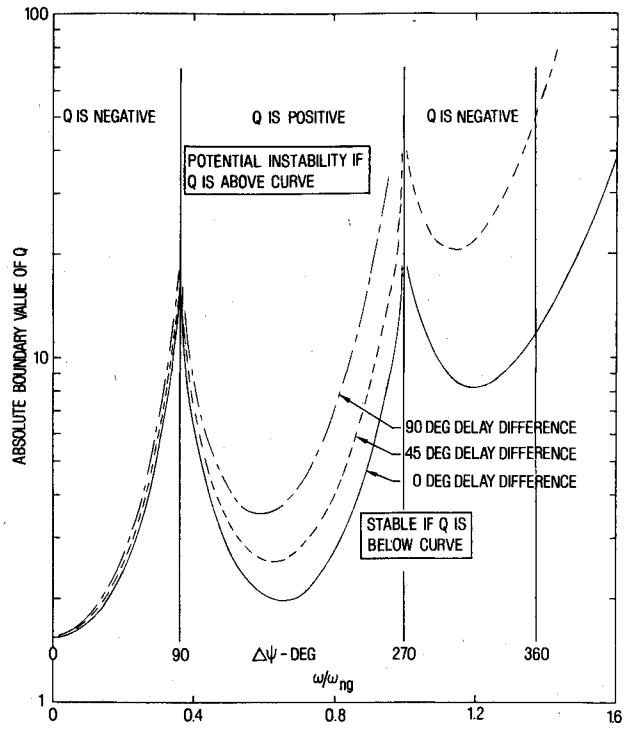

Fig. 3 Double-firing boundary chart.

a and b. If the value of Q for the system has the same algebraic sign as the boundary value of Q in that region, and if the absolute value of Q is greater than the boundary value plotted in Fig. 3, then a double-firing instability will occur if the worst-case disturbance torque is applied. If the absolute value of Q is less than the boundary value, then no double-firing instability can occur.

For a given structural damping and bending frequency, $\Delta\psi$ will increase with increases in rate gyro damping, filter time constant, or valve delays, or with a decrease in rate gyro natural frequency. A decrease in $\Delta\psi$ occurs for the reverse trends. Instability in the left-hand negative Q region, therefore, will tend to require a high-frequency lightly damped rate gyro with short filter time constant and valve delays. Instability in this region may be of practical concern for some systems, but for the systems studied by the author the left-hand region is of no interest because the values of Q are usually positive and $\Delta\psi$ is always greater than 90 deg. In the right-hand negative Q region, instability requires relatively low rate gyro frequencies and long filter and valve delays; however, the values of Q required for instability in the right-hand region are so large that instability in this region is probably not a matter of practical concern for any real system. The middle positive Q region is, however, of practical interest for the systems studied by the author. It is seen that the difference between on and off delays affects the curves significantly, and that the use of average delay gives an overly conservative boundary value (Q smaller than necessary) if the off delay is less than the on delay, as it usually is for real solenoid valves.

Acknowledgments

This work was supported by the Space and Missile Systems Organization of the Air Force Systems Command under Contract FO4701-78-C-0079.

References

[1] Hecht, C. and Loesch, F.C., "Work/Energy Analysis of Bending Limit Cycles in a Deadband Attitude Control System," *Journal of Spacecraft and Rockets*, Vol. 13, July 1976, pp. 406-415.

Method for Error Budgeting of Inertial Navigation Systems

Angus Andrews*
Rockwell International Science Center, Thousand Oaks, Calif.

Nomenclature

A,B	= general matrices of the same dimensions
C	= covariance matrix of a variate (denoted by subscript)
E	= expected-value operator
F	= $n \times n$ matrix as a function of time
G	= $n \times l$ matrix as a function of time
I	= identity matrix
i,j,k	= integers
l	= dimensions of the forcing noise vector u
m	= number of missions in rms performance estimates
n	= dimension of the modeled error state vector x
P	= matrix projecting x onto r or v (denoted by subscript)
Q	= lower-triangular matrix such that $Q^TQ = W$
R	= upper-triangular matrix such that $R^TR = C$
r	= position error vector
S	= upper triangular matrix = RQ^T
s,t	= time, $0 \le s \le t \le T$
T	= total time over which system performance is specified
$(\ )^T$	= transpose of a matrix or vector
trace	= sum of diagonal elements of a square matrix
u	= l-dimensional uncorrelated noise vector
v	= velocity error vector
W	= symmetrical weighting matrix
x	= n-dimensional state vector of the system error model
Φ	= $n \times n$ state transition matrix
ρ	= rate of increase of rms position error
0	= a submatrix of zeros

Introduction

ERROR covariance analysis has been used as a tool for determining the design requirements of inertial sensor systems.[1] It is a way of estimating overall system performance as a function of the performance of subsystems and components which contribute to system errors. Error budgeting requires solving the inverse problem, which is that of finding an allocation of allowable errors (error budget) among the subsystems such that the system meets a specified set of performance criteria. For inertial navigation and guidance systems, these performance requirements are usually specified in terms of such statistical quantities as the rms position or velocity errors, or the time-rate-of-growth of rms position errors.[2] A conventional approach for determining such statistics for a particular error budget is to integrate the matrix differential equations defining error covariance dynamics for the modelled system and mission, using the error budget to define the initial covariances and covariance dynamics. In order to define an error budget which meets the specified requirements, this process is repeated, using engineering judgement to adjust individual budget allocations

Received Dec. 19, 1978; revision received April 5, 1979.

Index categories: Analytical and Numerical Methods; Guidance and Control.

*Technical Staff, Mathematical Sciences Group, Physics and Chemistry Department.